Journal of Alloys and Compounds 512 (2012) 47–51

Contents lists available at SciVerse ScienceDirect

Journal of Alloys and Compounds

journal homepage: www.elsevier.com/locate/jallcom

Sol–gel preparation and characterization of NiCo and Ni_3Fe nanoalloys

P.Y. Li, J.A. Syed, X.K. Meng*

National Laboratory of Solid State Microstructures, Department of Materials Science and Engineering, Nanjing University, Nanjing 210093, People's Republic of China

ARTICLE INFO

Article history:
Received 2 July 2011
Received in revised form 31 August 2011
Accepted 3 September 2011
Available online 10 September 2011

Keywords:
Sol–gel
Nanoalloy
Order–disorder
Ferromagnetic

ABSTRACT

Sol–gel process is effective in preparation of metallic oxides. Here we report that sol–gel process based on chelating of citric acid is also effective in fabricating NiCo and Ni_3Fe nanoalloys under N_2 or H_2 atmosphere during heating treatment. With the introducing of surfactant, the average grain size of the nanoalloys is less than 10 nm and the grain size distribution is narrow. The formation of nanoalloys with equilibrium ordered phase rather than metastable disordered phase is confirmed by the occurrence of superlattice diffraction rings obtained by selected area electron diffraction. The Ni_3Fe nanoalloy shows typical ferromagnetic behavior at room temperature.

1. Introduction

Much attention has been paid to preparation and properties of binary nanoalloys due to their potential applications in electronics, engineering, catalysis, and medical fields [1,2]. Ni–Fe and Ni–Co alloys have been focused among researchers because of their useful magnetic properties, such as high saturation magnetization, high Curie temperature, and low coercive force [3–5]. These nanoalloys have been prepared by thermo-decomposition of organometallic precursors [3,6–12], co-reduction of metallic ions by hydrazine [13–15], magneto-sputtering [16], electrodeposition [17,18], and ball-milling [19–21]. For instance, thermo-decomposition of organometallic precursors, such as $Fe(acac)_3$ [3], $Co(acac)_2$ [3] (acac denotes acetylacetone), $Fe(CO)_5$ [6–8], $Co_2(CO)_8$ [7], $Ni(CO)_4$ [9], $Fe[\{N(SiMe_3)_2\}_2]$ (Me means methyl) [10], $Ni[(COD)_2]$(COD represents 1,5-cyclooctadiene) [10], $N(C_4H_9)_4)_3[Fe(CN)_6]$ [11], and $Co(\eta^3\text{-}C_8H_{13})(\eta^4\text{-}C_8H_{12})$[12] have been used to fabricate these nanoalloys with grain sizes less than 20 nm or even less than 10 nm. However, it is worth noting that these methods [3–15] have some shortcomings, for example, the organometallic precursors are relatively expensive and hydrazine and carbonyl complexes ($Fe(CO)_5$, $Co_2(CO)_8$, $Ni(CO)_4$) are highly toxic. Nontoxic agents have also been used to synthesis these nanoalloys [16–19] while the grain sizes of alloys prepared by these methods are larger than 20 nm. Therefore, it is necessary to develop a synthesis method to prepare these nanoalloys with grain size less than 10 nm using cheap and nontoxic chemical agents.

In Ni–Fe alloys, there are equilibrium ordered and metastable disordered phases where metastable disordered phase often occurs in alloys prepared by thermo-decomposition [9], magneto sputtering [15], and ball milling [18,19]. In order to prepare alloy with equilibrium ordered phase, post-annealing at high temperature is often required [15]. However, growth of grain size is often unavoidable during post-annealing at high temperature [22]. Therefore, it seems that equilibrium ordered phase is difficult to be directly obtained in Ni–Fe nanoalloy without post-annealing treatment.

In this work, we for the first time report that NiCo and Ni_3Fe nanoalloys with equilibrium ordered phase structure and grain size less than 10 nm can be directly prepared by traditional sol–gel process using cheap metallic nitrates, distilled water, citric acid, and surfactant. It is found that the use of chelating ligand of citric acid is essential in the formation of equilibrium ordered phase and the surfactant plays an important role in controlling grain size distribution of nanoalloys.

2. Experimental

The starting materials were cheap metallic nitrates, citric acid, distilled water, and sodium dodecyl sulfate (SDS). In a typical synthesis process, two metallic nitrates with stoichiometric atomic ratio (Ni:Co = 1:1, Ni:Fe = 3:1) were dissolved into distilled water. Then appropriate amount of SDS and citric acid were dissolved into the aqueous solution where the molar ratio of citric acid to total amount of metallic ions is 4:1. Dried gel was formed after the solution was stirred at 353 K for 1 h and dried at 383 K for at least one week. Then the dried gel was calcined at 600–700 K for different time under N_2 (for the preparation of NiCo nanoparticles) or H_2 atmosphere (for the preparation of Ni_3Fe nanoparticles). Black particles were obtained after cooling the calcined particles down to room temperature. For comparison, Ni–Co nanoalloy was also prepared from dried gel without SDS, and the as-prepared NiCo nanoalloys were referred to as Ni–Co-1 (with SDS) and Ni–Co-2 (without SDS) nanoalloys. Two Ni–Fe nanoalloys were also prepared by calcination

* Corresponding author. Tel.: +86 25 83685585; fax: +86 25 83595535.
E-mail address: mengxk@nju.edu.cn (X.K. Meng).

0925-8388/$ – see front matter © 2011 Elsevier B.V. All rights reserved.
doi:10.1016/j.jallcom.2011.09.007

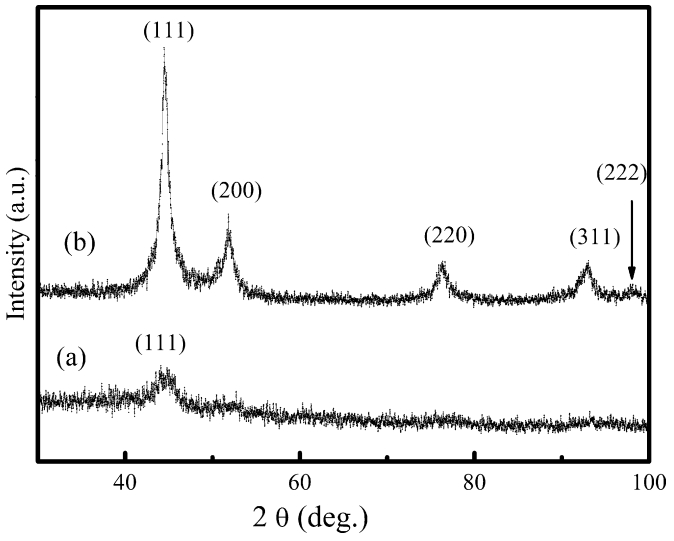

Fig. 1. The XRD analysis of Ni–Co-1 (a) and Ni–Fe-1 (b) ultrafine nanoparticles.

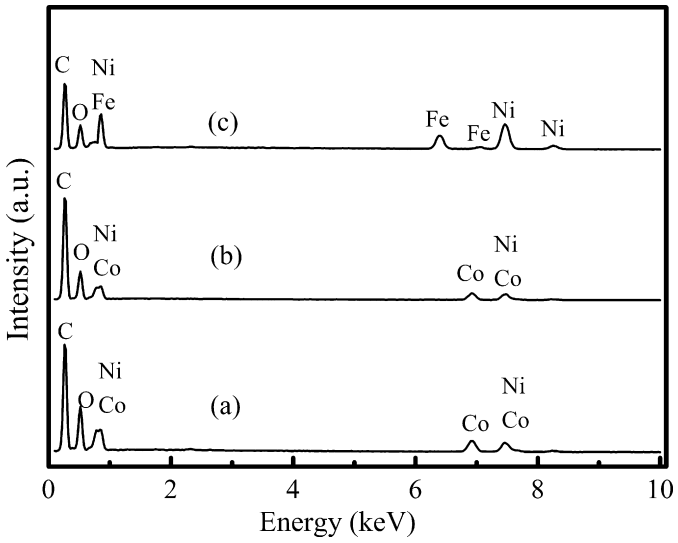

Fig. 2. The EDX results of Ni–Co-1 (a), Ni–Co-2 (b) and Ni–Fe-1 (c) nanoparticles.

of the dried gels at 600–700 K for 1.5 and 3 h, respectively. The two Ni–Fe nanoalloys were referred to as Ni–Fe-1 and Ni–Fe-2 nanoalloys.

The microstructure of as-prepared nanoparticles was analyzed by transmission electron microscope (TEM, JEM-2100) with an accelerating voltage of 200 kV and X-ray diffraction (XRD) using Cu K_α radiation with scanning rate of 2°/min. The elemental analyses of nanoalloys were recorded by energy dispersive X-ray spectroscopy (EDX, Oxford-2500) attached to a scanning electron microscope (SEM, S-3400). The magnetic property of Ni–Fe-1 nanoalloy was investigated by vibrating sample magnetometer (VSM, lakeshore, Model 7300 series) at room temperature where the magnetic field ranges from −1.5 T to 1.5 T. Furthermore, in order to make sure of the formation of Ni–Fe alloys and investigate order–disorder phase transition, Ni–Fe-1 nanoparticles were annealed at 973 K for 5 min under N_2 atmosphere followed by cooling down to room temperature, and then differential scanning calorimetry (DSC) measurement of the annealed particles was carried out on a STA-409 PC equipment from room temperature to 973 K under N_2 atmosphere with heating rate of 10 K/min.

3. Results and discussion

Fig. 1 shows the XRD analysis results of Ni–Co-1 (a) and Ni–Fe-1 (b) nanoparticles. In Fig. 1a, the (1 1 1) diffraction peak can be observed. In Fig. 1b, the (1 1 1), (2 0 0), (2 2 0), (3 1 1), and (2 2 2) diffraction peaks appear, which indicates that the as-prepared Ni–Fe particles have face-centered-cubic (FCC) phase structure. However, it is difficult to identify whether NiCo or Ni_3Fe nanoalloys form, because the lattice parameters of pure Ni, Fe, Co are very close to their corresponding alloys [16,23,24]. In addition, no diffraction peaks of oxidized phases such as NiO and Fe_2O_3 occur in Fig. 1b. This can be ascribed to small amount or poor crystallinity of NiO and Fe_2O_3.

Fig. 2 displays the EDX results of the Ni–Co-1 (a), Ni–Co-2 (b) and Ni–Fe-1 (c) nanoparticles. The signals of C, O, Ni, Co, and Fe can be observed in Fig. 2 and the corresponding atomic ratios of elements in Figs. 2a-c are 48.90:51.10 (Ni:Co), 50.95:49.05 (Ni:Co), and 75.41:24.59 (Ni:Fe), respectively. These ratios are in agreement with the initial ratios of two elements in starting metallic nitrates, indicating that the chemical composition of nanoparticles can be controlled by this sol–gel process. In addition, the occurrence of O signal results from the oxidization of the nanoparticles' surface, while C signal originates from the calcination of chemical agents such as citric acid at 600–700 K.

Fig. 3 shows TEM images of Ni–Co-1 (a and b), Ni–Co-2 (c and d), Ni–Fe-1 (e and f), Ni–Fe-2 (g–i) nanoparticles, typical selected area electron diffraction (SAED) results of the Ni–Co and Ni–Fe nanoparticles (j and k), respectively. It can be seen from Fig. 3a–h that nanoparticles with small grain sizes are supported by a kind of membrane, which can be reasonably assumed to be constructed by carbon. That the carbon element is assumed to exist in the as-prepared products is based on the following considerations. First, large molar ratio of citric acid to total amount of metallic ions (4:1) results in large amount of carbon during the calcination of the dried gel. Second, because the heating is in the temperature range of 600–700 K, the carbon element is bound to exist as it can only be eliminated at temperature higher than 800 K [25]. It is suggested that the carbon membrane is amorphous since no diffraction peaks associated with crystallized carbon is observed in the XRD result.

In Fig. 3a and b, the diameters of all particles are less than 10 nm and no aggregation of nanoparticles occurs. Moreover, the largest and smallest diameters are 9.62 and 2.50 nm, and the average grain size is 5.10 ± 1.0 nm. In Fig. 3c and d, the diameters of the majority grains are in the range of 3.81–7.62 nm. However, an abnormal large grain with diameter of 31.58 nm appears in Fig. 3c. These results indicate that the surfactant SDS plays an important role in controlling grain size distribution of the nanoparticles. In general, in liquid solution, SDS can disperse on the surface of grains. Therefore, repulsive force occurs in the surface of grains. As a result, grains are separated and the aggregation of particles is prohibited. SDS may decompose during the heating treatment. However, the completely removal of SDS can only take place at high temperature, e.g. higher than 723 K [26]. Because the heating temperature in our experiment is in the range of 600–700 K, it can be assumed that SDS does not decompose completely. That is to say, SDS remains in the calcined products. As a result, SDS disperses on the surface of nanograins, separates the nanograins and prevents aggregation of nanograins. In Figs. 3e–h, the shape of grains is spherical and the diameters for the majority of grains are smaller than 10 nm except that the diameter of one grain in Fig. 3e and three grains in Fig. 3g are larger than 10 nm. Based on statistics of grains in Figs. 3e–h, the average grain sizes of Ni–Fe-1 and Ni–Fe-2 nanoalloys are 7.00 ± 1.70 and 7.00 ± 1.86 nm, respectively. Fig. 3i displays high resolution transmission electron microscope (HRTEM) micrograph of Ni–Fe-2 nanoparticles where good crystallization can be observed. The interplanar spacing in Fig. 3i is 1.77 Å, corresponding to the (2 0 0) crystal plane of the nanoparticles. In order to make sure of the formation of nanoalloys, SAED measurements have been carried out and the corresponding results are shown in Figs. 3j and k where typical diffraction rings of (1 1 1), (2 0 0), (2 2 0), and (2 2 2) reflection planes can be observed. Moreover, the diffraction rings of (2 1 1) superlattice reflection plane can also be observed in Figs. 3j

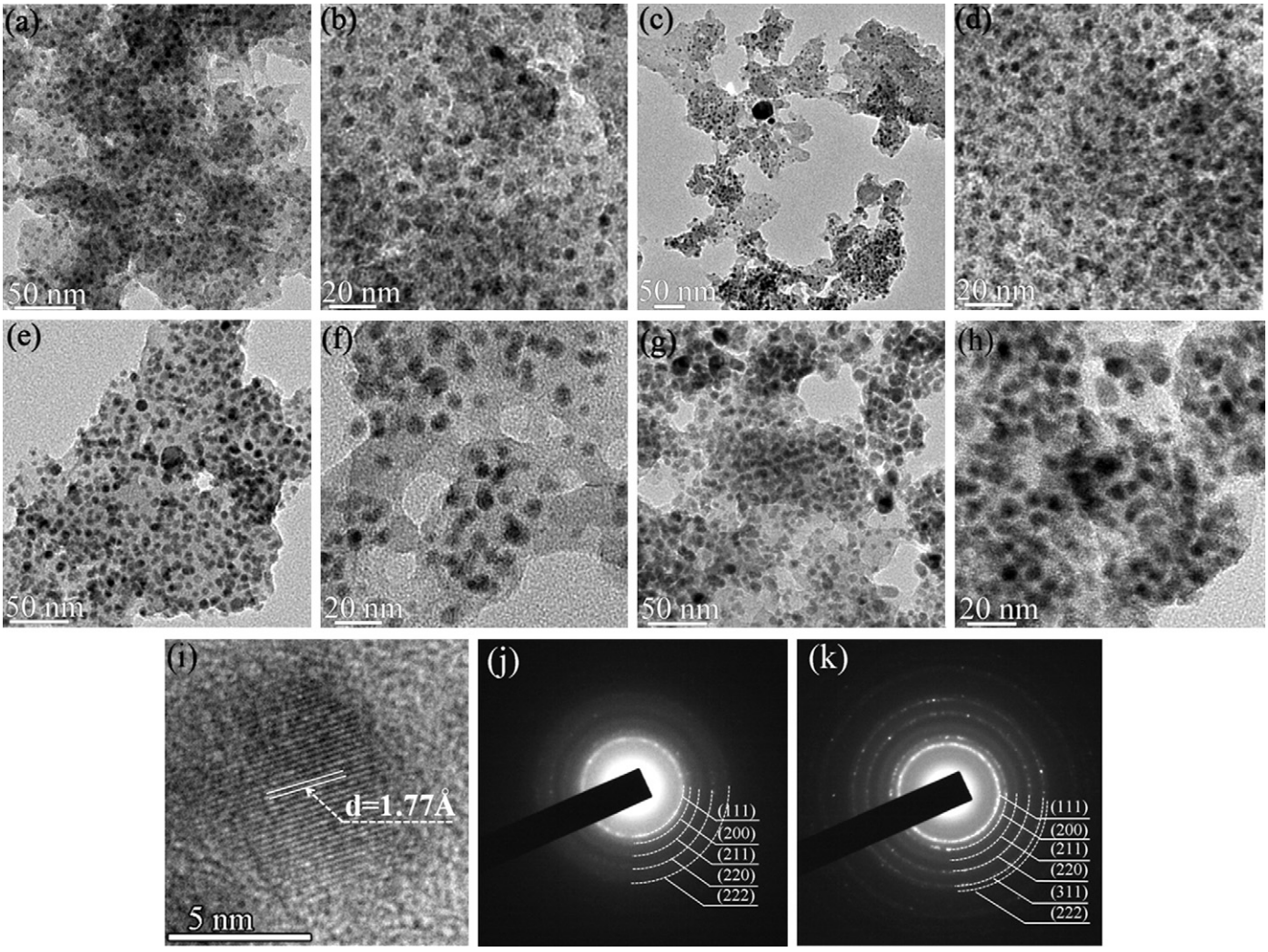

Fig. 3. The TEM images of Ni–Co-1 (a and b), Ni–Co-2 (c and d), Ni–Fe-1 (e and f), Ni–Fe-2 (g–i), typical SAED results of Ni–Co (j), and Ni–Fe (k) nanoparticles. Panel (i) shows a high-resolution transmission electron microscope (HRTEM) image of Ni–Fe-2 nanoparticles.

and k, indicating the formation of equilibrium ordered phase in NiCo and Ni_3Fe nanoalloys.

Fig. 4 shows hysteresis loop of Ni–Fe-1 nanoalloy at room temperature. It can be seen from Fig. 4 that the magnetization is saturated when the magnetic field is in the range of 5000–10,000 Oe and −10,000 to −5000 Oe, showing typical ferromagnetic behavior of the nanoalloy at room temperature. The saturation magnetization (M_S) at room temperature of the nanoalloy is 12.23 emu/g, as shown in Fig. 4. The M_S is much lower than its counterpart in coarse-grained (cg) Ni_3Fe alloy [27,28]. This is in agreement with the general tendency of ferromagnetic nanocrystals where magnetization at room temperature of nanocrystals decreases as the average grain size decreases [29,30]. According to bond order-length-strength correlation mechanism, the depression of M_S originates from decreasing of spin-spin exchange energy in nanocrystals due to the coordination number imperfection of atoms near or at surface of nanocrystals [31]. The percent of atoms near or at surface increases as the grain size is decreased. As a result, decreasing of spin–spin exchange energy occurs and then M_S decreases due to decreases in average grain size.

Based on the results described above, it is claimed that NiCo and Ni_3Fe nanoalloys with equilibrium ordered phase can be directly prepared by sol–gel process. This phenomenon is of particular interest noted that alloys prepared by other methods usually have

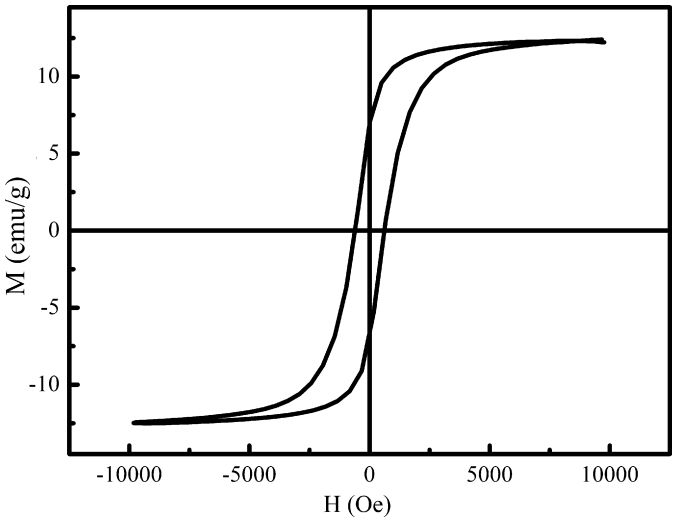

Fig. 4. The hysteresis loop of Ni–Fe-1 nanoalloy at room temperature.

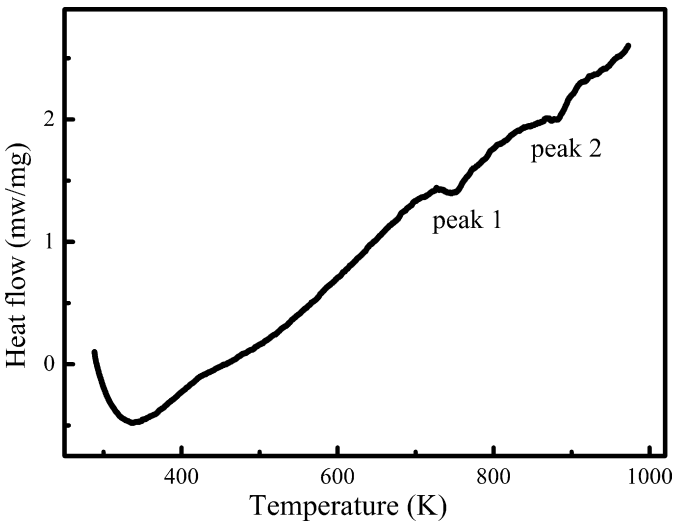

Fig. 5. The DSC measurement result of Ni_3Fe alloy after the Ni–Fe-1 nanoalloy has been annealed at 973 K for 5 min followed by cooling down to room temperature.

disordered phase. Here we propose that the direct formation of ordered phase is due to the utilization of citric acid. In general, chemical agents are homogeneously mixed in the presence of citric acid since it can chelate with metallic ions [32–34]. In our experiments, the molar ratio of citric acid to metallic ions is 4:1. With small amount of citric acid, it is well known that some part of citric acid coordinates with one type of metallic ion while the remaining citric acid coordinates with another type of metallic ion. On the contrary, with large amount of citric acid (our work), citric acid coordinates with one type of metallic ion and the excess amount of citric acid coordinates with another type of metallic ion simultaneously. As a result, the two metallic ions distribute homogeneously in the dried gel, and the form of "single molecular" in dried gel becomes possible. No interface exists between the two metallic elements. In other words, only short-range diffusion of atoms is required for the formation of alloys during calcination process. In addition, it is well known that high diffusion rates of atoms occur in nanocrystalline materials [35]. Ordered phase of nanoalloys can thus be obtained by this sol–gel process under N_2 or H_2 atmosphere. However, in other methods such as arc-melting [4,5], thermo-decomposition of organometallic precursors [6–12], and ball milling [18,19], the chemical agents are not "bonded", and interface often appears between phases containing two metallic elements. Therefore, long-range diffusion of atoms across interface is often required in order to form alloys. Nanoalloys with disordered phase are easily obtained by these methods. Although the post-annealing is often required in order to prepare alloys with ordered phase structure, it is not necessary for the preparation of nanoalloy with ordered phase structure by sol–gel process.

In Ni–Fe alloys, chemical ordering phase transition is often observed during the post-annealing of Ni–Fe alloys [16,20,36]. Here we report that chemical disordering phase transition also occurs in Ni_3Fe alloy. Fig. 5 shows the DSC result of Ni_3Fe alloy where the alloy has been obtained by annealing the Ni–Fe-1 nanoalloy at 973 K for 5 min followed by cooling down to room temperature. In Fig. 5, an upward peak denotes an exothermal process. Two endothermal peaks, referred to as peaks 1 and 2, can be observed in Fig. 5 with peak temperatures being 750 and 885 K, respectively. These two peaks should not connect with grain growth because an exothermal process often associates with grain growth [37]. However, the temperatures of the two peaks are in agreement with those of order–disorder and Curie transition temperatures (773 and 863 K) in cg Ni_3Fe alloy [38]. Since the Ni_3Fe alloy measured by DSC has been prepared from annealing the Ni–Fe-1 nanoparticles at 973 K, the grain size of annealed alloy is considered to be in micrometer range. Therefore, it is suggested that the two peaks should originate from order–disorder transition and Curie transition of Ni_3Fe alloy. Moreover, peak 1 is connected with an endothermal phase transition process, indicating that peak 1 should originate from the chemical disordering (order → disorder) phase transition because an endothermal process is involved in chemical disordering phase transition while an exothermal process is involved in chemical ordering (disorder → order) phase transition in Ni_3Fe alloy. This result means that fully ordered Ni_3Fe alloy can be prepared otherwise chemical ordering phase transition should take place during the DSC measurement. This result is also contrary to our previous result of chemical ordering transition in Ni_3Fe nanoalloy prepared by electrodeposition where an exothermal peak occurs [20]. This is because the Ni_3Fe nanoalloy prepared by electrodeposition is only partially ordered. In addition, the occurrence of the endothermal peak 2, originating from Curie transition, is also contrary to previous opinion that Curie transition in Ni–Fe alloys is of second order character [39]. However, the occurrence of the endothermal peak 2 is in agreement with the fact that endothermal peaks associated with Curie transition in Fe, Co, and Ni can be observed during DSC measurements [40]. Since there is no consensus about the intrinsic character of Curie transition, interpretation of the disagreement between our result and previous opinion is beyond the scope of this article.

4. Conclusions

In summary, we have shown that sol–gel process can be used to fabricate equilibrium ordered NiCo and Ni_3Fe nanoalloys with grain size less than 10 nm by using cheap and nontoxic inorganic chemical agents. N_2 or H_2 atmosphere is necessary for the preparation of nanoalloy. The occurrence of ordered phase is associated with the "bonding effect" of the chelating ligand of citric acid. The sol–gel method is a useful way to prepare nanoalloys with equilibrium ordered phase. It is expected to have broad applications in metallic field.

Acknowledgements

This work was jointly supported by the PAPD, the Fundamental Research Funds for the Central Universities, the Open Foundation of Key Laboratory of Automobile Materials, the Opening Project of Jiangsu Key Laboratory of Advanced Metallic Materials, the National Natural Science Foundation of China, and the State Key Program for Basic Research of China.

References

[1] W.S. Seo, J.H. Lee, X.M. Sun, Y. Suzuki, D. Mann, Z. Liu, M. Terashima, P.C. Yang, M.V. Mcconnel, D.G. Nishimura, H.J. Dai, Nat. Mater. 5 (2006) 971–976.
[2] R. Ferrando, J. Jellinek, R.L. Johnston, Chem. Rev. 108 (2008) 845–910.
[3] G.S. Chaubey, C. Barcena, N. Poudyal, C.B. Rong, J.M. Gao, S.H. Sun, J.P. Liu, J. Am. Chem. Soc. 129 (2007) 7214–7215.
[4] R.S. Sundar, S.C. Deevi, Int. Mater. Rev. 50 (2005) 157–192.
[5] T. Sourmail, Prog. Mater. Sci. 50 (2005) 816–880.
[6] C. Desvaux, C. Amiens, P. Fejes, P. Renaud, M. Respaud, P. Lecante, E. Snoeck, B. Chaudret, Nat. Mater. 4 (2005) 750–753.
[7] M. Zubris, R.B. King, H. Garmestani, R. Tannenbaum, J. Mater. Chem. 15 (2005) 1277–1285.
[8] F. Dumestre, S. Martinez, D. Zitoun, M.C. Fromen, M.J. Casanove, P. Lecante, M. Respaud, A. Serres, R.E. Benfield, C. Amiens, B. Chaudret, Faraday Discuss. 125 (2004) 265–278.
[9] F.D. Ge, L.M. Chen, W.J. Ku, J. Zhu, Nanostruct. Mater. 8 (1997) 703–709.
[10] O. Margeat, D. Ciuculescu, P. Lecante, M. Respaud, C. Amiens, B. Chaudret, Small 3 (2007) 451–458.
[11] B. Folch, J. Larionova, Y. Guari, L. Datas, C. Guérin, J. Mater. Chem. 16 (2006) 4435–4442.

[12] C. Desvaux, F. Dumestre, C. Amiens, M. Respaud, P. Lecante, K. Snoeck, P. Fejes, P. Renaud, B. Chaudret, J. Mater. Chem. 19 (2009) 3268–3275.
[13] Q.L. Liao, R. Tannenbaum, Z.L. Wang, J. Phys. Chem. B 110 (2006) 14262–14265.
[14] Y.D. Li, L.Q. Li, H.W. Liao, H.R. Wang, J. Mater. Chem. 9 (1999) 2675–2677.
[15] L.J. Liu, J.G. Guan, W.D. Shi, Z.G. Sun, J.S. Zhao, J. Phys. Chem. C 114 (2010) 13565–13570.
[16] Q. Zeng, I. Baker, Y. Zhang, IEEE. Trans. Magn. 41 (2005) 3358–3360.
[17] P.Y. Li, H.M. Lu, Z.H. Cao, S.C. Tang, X.K. Meng, X.S. Li, Z.H. Jiang, Appl. Phys. Lett. 94 (2009) 213112.
[18] H.Q. Li, P.K. Liaw, H. Choo, A. Misra, Appl. Phys. Lett. 93 (2008) 051907.
[19] V. Pop, O. Isnard, I. Chicinas, J. Alloys Compd. 361 (2003) 144–152.
[20] Z. Sparchez, I. Chicinas, O. Isnard, V. Pop, F. Popa, J. Alloys Compd. 434–435 (2007) 485–488.
[21] W. Wang, J.G. Guan, S.L. Zhao, Q.X. Zhang, J. Wuhan Univ. Technol. 21 (2006) 16–18.
[22] P.Y. Li, H.M. Lu, Z.H. Jiang, Y.N. Huang, X.K. Meng, J. Phys. D: Appl. Phys. 44 (2011) 135402.
[23] Y.W. Jiang, S.G. Yang, Z.H. Hua, H.B. Huang, Angew. Chem. Int. Ed. 48 (2009) 8529–8531.
[24] J.W. Drijver, F.V.D. Woude, S. Radelaar, Phys. Rev. B 16 (1977) 985–992.
[25] J. Lin, M. Yu, C.K. Lin, X.M. Liu, J. Phys. Chem. C 111 (2007) 5835–5845.
[26] T.W. Wang, O. Sel, I. Djerdj, B. Smarsly, Colloid. Polym. Sci. 285 (2005) 1–9.
[27] R.S. Tebble, D.J. Caraik, Magnetic Materials, Wiley-Inter Science, 1969.
[28] X.W. Wei, G.X. Zhu, Y.J. Liu, Y.H. Ni, Y. Song, Z. Xu, Chem. Mater. 20 (2008) 6248–6253.
[29] C.Q. Sun, Prog. Solid State Chem. 35 (2007) 1–159.
[30] Q. Jiang, H.M. Lu, Surf. Sci. Rep. 63 (2008) 427–464.
[31] W.H. Zhong, C.Q. Sun, S. Li, Solid State Commun. 130 (2004) 603–606.
[32] F. Peng, G.Z. Li, X.X. Liu, S.Z. Wu, Z. Tong, J. Am. Chem. Soc. 130 (2008) 16166–16167.
[33] G. Liu, Y. Liu, G. Yang, S.Y. Li, Y.H. Zu, W.X. Zhang, M.J. Jia, J. Phys. Chem. C 113 (2009) 9345–9351.
[34] S. Mathur, M. Veith, R. Rapalaviciute, H. Shen, G.F. Goya, W.L.M. Filho, T.S. Berquo, Chem. Mater. 16 (2004) 1906–1913.
[35] L. Lu, M.L. Sui, K. Lu, Science 287 (2000) 1463–1466.
[36] C.N. Chinnasamy, A. Narayanasamy, N. Ponpandian, K. Chattopadhyay, M. Saravanakumar, Mater. Sci. Eng. A 304–306 (2001) 408–412.
[37] G.D. Hibbard, K.T. Aust, U. Erb, Acta Mater. 54 (2006) 2501–2510.
[38] X. Jiang, G.E. Ice, C.J. Sparks, L. Robertson, P. Zschack, Phys. Rev. B 54 (1996) 3211–3226.
[39] I.V. Vernyhora, D. Ledue, R. Patte, H. Zapolsky, J. Magn. Magn. Mater. 322 (2010) 2465–2470.
[40] S. Yang, X.B. Ren, X.P. Song, Phys. Rev. B 78 (2008) 174427.